doi:10.1111/j.1460-2695.2005.00948.x

A refined CLNA model in fretting fatigue using asymptotic characterization of the contact stress fields

M. CIAVARELLA[1] and D. DINI[2]

[1] *CEMeC Centro di Eccellenza in Meccanica Computazionale Politecnico di Bari, V.le Gentile 182, 70125 Bari, Italy,*

[2] *Department of Engineering Science, University of Oxford, Parks Road, OX1 3PJ, Oxford, UK*

Received in final form 9 August 2005

ABSTRACT Using the Atzori–Lazzarin criterion, the first author has recently proposed a unified model for fretting fatigue (FF), called the crack-like notch analogue (CLNA) model. Two possible types of behaviour were suggested: either 'crack-like' or 'large blunt notch,' and these are immediately studied in the typical condition of constant normal load and in phase oscillating tangential and bulk loads. The former condition ('crack-like') was treated by approximating the geometry to the perfectly flat one of the crack analogue (CA), improved in some details, reducing all possible geometries to a single contact problem. The latter ('large blunt notch'), with a simple peak stress condition i.e. a simple notch analogue model. In the present paper, the calculation of the 'crack-like' behaviour is improved using the recent asymptotic characterisation developed by Dini, Hills and Sackfield, which extracts the asymptotic singular stress field of the fretting contact. A significant difference is found in the 'equivalent' geometric factor obtained for the Hertzian geometry, particularly near full sliding, where the new criterion is more conservative, but still not large enough to permit to find, for example in Nowell's FF experimental data, if the refinement is an improvement of predictive capabilities. In flatter geometries, the difference is expected to be even smaller than in the case of the Hertzian geometry, and in this case, the original CLNA model, for its simplicity, remains a very convenient simple closed form criterion.

Keywords fretting fatigue; HCF fatigue; safe-life design.

NOMENCLATURE

a = crack half-width
a^* = transitional size between 'crack-like' and 'notch-like' behaviour
a_0 = El Haddad 'intrinsic crack size'
a_c = transitional size between 'crack-like' and 'notch-like' behaviour for Lucàs-Kesnil
b = contact half-width
c_H = Heywood material constant
c_N = Neuber material constant
c_P = Peterson material constant
d = partial slip contact size
E = Young's modulus
f = coefficient of friction
k = geometrical contact factor
K_f = strength reduction factor for notched specimens
K_{ff} = fretting strength reduction factor
K_{ft} = fretting stress concentration factor
K_P = generalised mode I stress intensity factor

Correspondence: M. Ciavarella. E-mail: mciava@poliba.it

K_Q = generalised mode II stress intensity factor
K_t = Stress concentration factor
p = pressure
$\overline{p}$ = average pressure
P = normal load
p_0 = peak pressure
q = shear traction
$\overline{q}$ = average shear traction
Q = tangential load
t = local coordinate for the asymptotic solutions
$\boldsymbol{\nu}$ = Poisson's ratio
Y = geometrical factor for normal cracks
Y_{FF} = original CLNA equivalent geometrical factor
$Y_{FF,\,Dini}$ = refined CLNA equivalent geometrical factor
$Y_{FF,\,slip}$ = original CLNA equivalent geometrical factor—slip
$Y_{FF,\,stick}$ = original CLNA equivalent geometrical factor—stick
γ = body compliance factor
σ_b = remote bulk stress
σ_{con} = stress induced by the contact
σ_{max} = maximum axial stress
σ_y = axial stress
ΔK_{th} = long crack stress intensity threshold
$\Delta\sigma$ = fatigue limit

INTRODUCTION

Background

The Atzori–Lazzarin[1] criterion has recently been used by Ciavarella[2] within the context of fretting fatigue. The Atzori–Lazzarin criterion obtains the strength reduction factor for notched specimens in fatigue, K_f, in specimen with cracks, or blunt and sharp notches, as the minimum between the stress concentration factor K_t, and the 'crack-like' strength reduction factor, written in the most general case including geometrical factors (Atzori *et al.*[3])

$$K_f = \begin{pmatrix} \sqrt{1+Y^2\dfrac{a}{a_0}}, & \text{for} \quad a < a^* \\ K_t, & \text{for} \quad a > a^* \end{pmatrix} \quad \text{or}$$

$$K_f = \text{Min}\left(\sqrt{1+Y^2\frac{a}{a_0}}, K_t\right), \tag{1}$$

where a is the crack half-width for an internal crack, or the width for an edge crack (see also Fig. 1), Y is the geometrical factor correcting with respect to the ideal case of central crack in a infinite plate. The transition from uncracked material to long crack (or crack-like notch) occurs at the size a_0/Y^2 defined as a function of the size a_0, which in turn is sometimes denominated 'intrinsic crack size' (ElHaddad *et al.*[4]),

$$a_0 = \frac{1}{\pi}\left(\frac{\Delta K_{th}}{\Delta\sigma_1}\right)^2, \tag{2}$$

where ΔK_{th} is threshold stress intensity range and $\Delta\sigma_1$ fatigue limit range of the material.

Similarly, a^* is the transitional size where the 'crack-like notch' behaviour gives place to the 'large blunt notch' behaviour*

$$a^* = \frac{a_0}{Y^2}K_t^2, \tag{3}$$

i.e. this size is K_t^2 times larger than the size a_0/Y^2. This clearly indicates that for large enough stress concentration factors K_t, the size becomes extremely large and it is not easy to observe in practice (which explains the widespread use of standard linear elastic fracture mechanics (LEFM) even if at every crack tip there is always some degree of blunting).

It is interesting to note the generality of the proposed approach. Ciavarella and Meneghetti[5] have, for example, recently compared the Atzori–Lazzarin[1] criterion with classical formulations for the fatigue strength reduction factor of notched specimen, K_f, such as those by Neuber, Peterson and Heywood, which were developed long before fracture mechanics, and hence their material constants (c_P, c_N, c_H, respectively) were originally connected with the material's tensile strength only. They also attempted a more refined criterion that was capable of dealing with the abrupt transition in the Atzori–Lazzarin criterion in the region of transition from long crack threshold

*For $Y^2a^* \gg a_0$

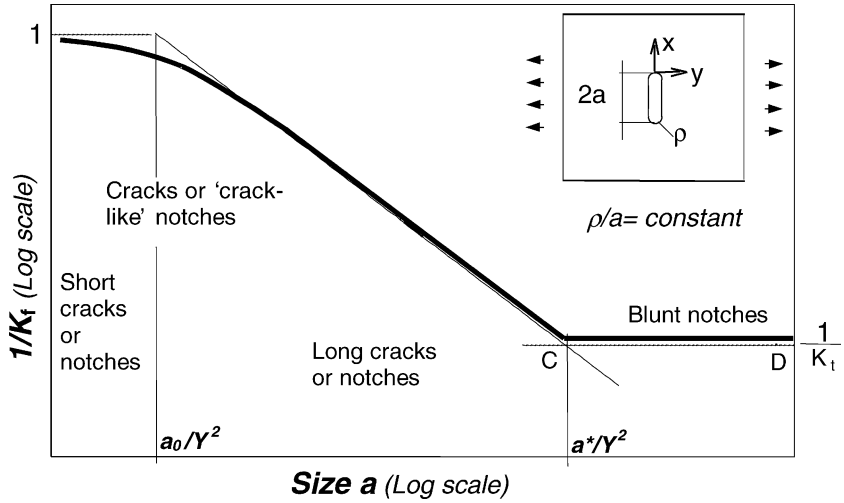

Fig. 1 Schematic of the Atzori–Lazzarin[1,3] criterion (indicated with a bold solid line), Eq. (1).

to blunt notch behaviour (point C in Fig. 1) is unlikely to be justified experimentally. In particular, they introduced in this region the Lukàs–Klesnil criterion, having a sound interpretation in terms of self-arrested cracks ahead of a rounded notch for which the Creager–Paris stress field is valid, noting that this criterion has a very smooth link to the El Haddad branch of the curve at the size a_c which is readily seen to be

$$a_c = \frac{a_0}{Y^2}(K_t - 1). \tag{4}$$

However, a large number of notches-related experimental data taken from the literature were examined in Ciavarella and Meneghetti,[5] showing no significant advantage of the new criterion over the Atzori–Lazzarin[1] criterion. Moreover, while in general there is no special reason to prefer one over the other, the greater simplicity of the Atzori–Lazzarin[1] criterion turns out particularly helpful in the case of fretting fatigue, since it permits evaluation of the effect of fretting using either a crack or notch analogue. This implies that either a contact stress intensity factor or a contact stress concentration factor is required to predict fretting thresholds, avoiding the need to compute an internal stress field induced by the contact/fatigue loading interaction. This is a very important result, considering that most of the present alternative lifing approaches seem to require the knowledge of the full stress field in order for fretting thresholds to be assessed.

Extension of the model to fretting fatigue

Let us consider a fretting fatigue (FF) test configuration. The cylindrical indenter pressed against a plane specimen (see Fig. 2) is the prototypical example used to study fretting problems, and it is also convenient as an example of very remote geometry from the flat indenter. If the specimen thickness is much larger than the contact width,

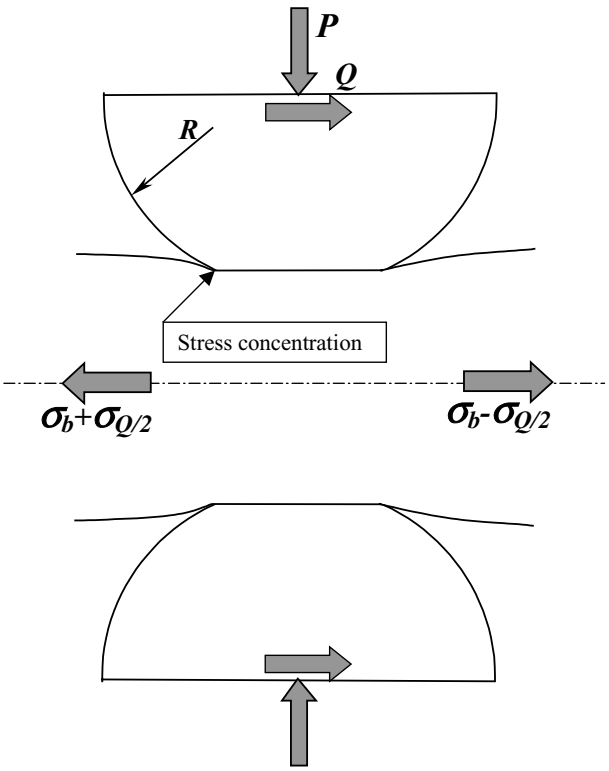

Fig. 2 Fretting fatigue test configuration.

half-plane theory can be applied for the solution of the problem. A well-known result among fretting researchers is that in such (or similar) configurations, contact loading induces a stress concentration with the half-plane, without the half-plane being a proper geometrical notch. A limit case is when the shape of the indenter is sharp ended and the stress field at the edge of the contact is singular. In that case, as suggested with the MIT so-called *crack analogue* (*CA*) *model*,[6] it is relatively easy to see the connection with LEFM, because the contact-induced singularity has

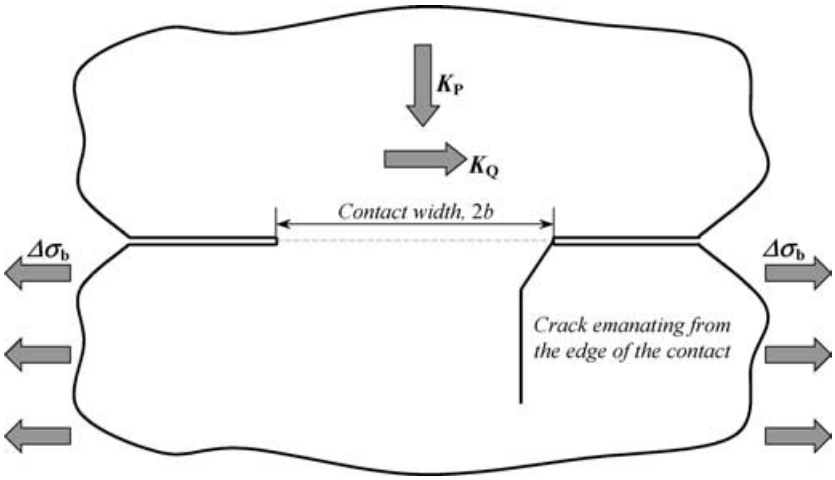

Fig. 3 The so-called *crack analogue (CA) model*,[6] where a fretting fatigue contact is approximated with an external crack under oscillating generalised mode II, K_Q (the generalised mode I, K_P, is neglected because it is constant and also because it is negative).

exactly the same form as crack-induced singularity. Obviously, the equivalent fretting mode I loading (induced by the normal compressive force P) may now be considered as an obstacle for crack propagation. Therefore, in most cases, the FF effect is due to mode II singularity, or to mixed mode (Fig. 3).

The 'crack-like' together with the 'notch-like' behaviour (typical of large contacts characterised by weaker stress gradients) are both taken into account within the CLNA model.[2] In particular, for the crack-like behaviour, the simplest path is followed, namely to approximate the geometry altogether with a flat and sharp geometry, thereby obtaining the reduction of all possible contact configurations to a single, well-know case, which in turn is solved for once and then gives the CLNA model independent on geometry in this range. The other possible range, that of stress concentration factor, remains geometry dependent. Here, we should just point out that the crack analogy could be only used as an approximation when applied to study some fretting configurations. Difficulties may arise from the fact that no perfectly sharp geometry or no exact square root singularity is achieved in practical FF conditions, whereas cracks are sharp because they arise naturally by initiation. Moreover, the contact pressure in general goes to zero at the edges (any real contact shows in fact some rounding at the edges of the contact), and consequently Coulomb friction also predicts bounded shear tractions. Hence, one may wonder if there could be alternative, more refined calculations of the stress field when a non-sharp geometry is concerned, to compute the equivalent stress singularity induced. Dini, Hills and Sackfield[7,8] recently did a detailed analysis of the contact stress field, dividing its local asymptotic values into a generalised stress intensity factor contribution, and a local perturbation: this permits to find an alternative extraction of the equivalent stress intensities, which we here call 'refined.' However, it should be borne in mind that, 'refined' here means that we extract the stress intensities from the actual stress field, rather than from an approximation of the geometry (as in the original CLNA model), but eventually we will only use either the stress intensities or the stress concentrations as parameters entering into the fatigue model, and hence the characterisation will remain approximate from an experimental point of view. In fact, since and only experimental investigations can confirm the independence on geometry of the 'crack-like' regime predicted by CLNA, or the mild dependence, expected in the 'refined' model. In fact, the crack-like regime is essentially based on the idea that cracks will self-arrest at a size large enough to neglect local differences in the stress field in the absence of the crack. Hence, the answer in general depends on subtle competition between length scales associated to either the stress field or to the crack size. Notice that in the contact case, length scales are not immediately defined as in the case of the notch, as friction induces an additional length scale in the stick-slip transition region. Detailed experimental comparisons and test cases would be extremely expensive and difficult to conduct, and hence it remains simpler to ascertain how large the difference between the two models can be, in order to have a better understanding, and perhaps plan experiments in the regions where the differences are largest.

Refined method based on asymptotics

To study the contact singularity in detail, Dini, Hills and Sackfield[7,8] wrote a general solution for the stress field expansion in the contact loading configuration of tangential and bulk stress oscillating in phase, with normal load kept constant. The results can be applied to *any* 'bounded' problem: this means that a generalised stress intensity factor for complete contacts can be used to characterise the 'crack-like' behaviour described in the CLNA model. The

expansion works like in the Creager and Paris equation for a rounded crack, i.e. such that intrinsic length scales in the stress fields are retrieved, and the corresponding equivalent singular stress field found.

It should be noted that the FF reduction of strength factor, K_{ff}, in the CLNA model is the ratio between fatigue limit and bulk stress load. For the 'crack-like' model part, the contact loadings *largely* affect the value of the equivalent geometrical factor of Eq. (1). For the 'blunt notch' model part, the contact loading, again, *largely* affects the exact value of the peak stress, and the two dependencies are not exactly similar. Therefore, the combined effects result in a complicated dependence of the transition size (equivalent to a^* in the crack–notch analogy), from loading condition.

The scope of the present paper is to incorporate the findings of Dini, Hills and Sackfield within the CLNA model, in particular comparing the resulting prediction of the 'crack-like' behaviour with the simplified account in the original CLNA model.

THE ORIGINAL CLNA MODEL

A generic FF problem is a much more complex situation than the standard geometric notch or crack subject to a remote uniaxial tensile fatigue loading. For a 'remote stress' condition (equivalent to the tensile stress in uniaxial fatigue) we could consider the bulk load, σ_b, the contact pressure, p, or the shear traction, q. There might also be various mode singularities (possibly mode I, II and III) under non-proportional loading. However, by limiting our attention to constant normal load and oscillating tangential load, the most significant contribution to fatigue life corresponds to oscillating axial stresses induced by the remote bulk load.

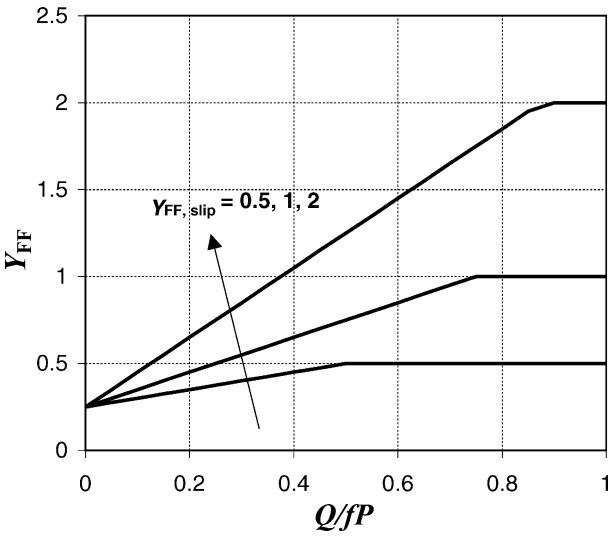

Fig. 4 The fretting fatigue CLNA *fictitious geometrical factor* Y_{FF}, given by the minimum between $Y_{FF, slip}$ and $Y_{FF, stick}$ from Eq. (6).

Considering the fretting pad as a square-ended foot pressing over a fatigue specimen, for a constant mode I normal load P, and a varying mode II load Q, the appropriate stress intensity factors (SIFs) were obtained without considering the details of the contact problem (for a 2D geometry and a $R = -1$ loading ratio). Mean pressure and mean shear traction, $\overline{p} = \frac{P}{2b}$ and $\overline{q} = \frac{Q}{2b}$, respectively, were considered by Ciavarella and Macina[9] as main loading parameters, Dundurs' mismatch constant, β, was assumed to be zero, and half-plane elasticity was used for both materials. Notice that this is rigorously valid only in the case of a rigid punch indenting an incompressible material, i.e. when $E_1 \to \infty$ and $\nu_1 \to 1/2$, and the constant $\gamma \to 1$, where

$$\gamma = \left(\frac{E_2^*}{E_1^*} + 1\right) = \left(\frac{\left(1 - \nu_1^2\right) E_2}{E_1\left(1 - \nu_2^2\right)}\right) + 1. \tag{5}$$

The extension of the Atzori–Lazzarin diagram to fretting is achieved by defining Y_{FF}, a *fictitious geometrical factor*. As already stated above, Y is normally used to include geometrical effects with respect to the classical central crack in the infinite plate solution. In the CLNA model, the mode II SIF has been written in terms of the bulk stress and the factor Y_{FF}, differently from a true geometrical factor in standard fracture mechanics, is here a factor depending on loading conditions (the dependence on contact geometry is also considered in the original model using a contact geometrical factor but this is not discussed in this paper).[2] Specifically, considering Hertzian contacts, the resulting *fictitious geometrical factor* is the minimum between

$$Y_{FF, stick}\left(\sigma_b, \overline{p}, \frac{Q}{P}\right) = \frac{2}{\pi}\frac{\overline{p}}{\sigma_b} Q/P + \frac{1}{2\gamma}$$

$$Y_{FF, slip}\left(\sigma_b, \overline{p}, f\right) = \frac{2}{\pi}\frac{f\overline{p}}{\sigma_b}. \tag{6}$$

The improvement over the original MIT so-called *CA model*[6] is larger for large bulk loads and low Q/fP, when the effect of bulk load dominates over the tangential load, i.e. away from the frictional limit behaviour, which is obtained for relatively large values of Q/fP. The resulting minimum value of Y_{FF}, $\min(Y_{FF})$ is plotted in Fig. 4, for three example cases. Here, $\gamma = 2$ (i.e. elastically similar contacts) as it is clear from the starting point of the curves on the plot, and the limit values are chosen as $Y_{FF, slip} = 0.5,1,2$. Notice that the point of transition from Eq. (6) is

$$\frac{Q}{fP} Y_{FF, slip} + \frac{1}{4} = Y_{FF, slip}, \tag{7}$$

and therefore it occurs at $\frac{Q}{fP} = 0.5, 0.75, 0.875$, respectively. By introducing the definition of $\min(Y_{FF})$ into the crack-like part of Eq. (1) (i.e. that for $a < a^*$ in Fig. 1 for the equivalent crack–notch problem), we obtain the FF strength reduction factor as

$$K_{ff}\left(\frac{\overline{p}}{\sigma_b}, \frac{Q}{P}; f, \frac{b}{a_0}\right) = \sqrt{1 + \left\langle \frac{2}{\pi}\frac{\overline{p}}{\sigma_b}\frac{Q}{P} + \frac{1}{2\gamma}; \frac{2}{\pi}\frac{\overline{p}}{\sigma_b} f \right\rangle^2 \frac{b}{a_0}}, \quad (8)$$

where $<A; B>$ indicates the minimum between A and B. Notice that K_{ff} in the final form of Eq. (8) depends on three non-dimensional factors only: the pressure ratio $\frac{\overline{p}}{\sigma_b}$, *either* the load ratio Q/P *or* the friction coefficient f, and the contact width ratio, b/a_0. One comment could be added to this discussion by noting that the factor Y_{FF} is generally a geometrical factor and, hence, is usually $Y_{FF} > 1$. Here, since Y_{FF} takes into account of many loading factors, it can be much lower than *one* as indeed in the example case of Fig. 4, and particularly for low values of Q/fP when the lower limit is due mainly to the constant γ induced by the bulk stress not being symmetrical in the contacting pair of materials. This was explained in detail by Ciavarella and Macina.[10]

REFINED MODEL: FORMULATION

A refined solution for the *fictitious geometrical factor* for incomplete contacts can be obtained by characterising pressure and shear traction distributions by the means of local asymptotic solutions as developed by Dini, Hills and Sackfield.[7,8] First, it should be stated that this set of solutions are intended to describe, fully, the state of stress adjacent to the *edge* of a general incomplete contact suffering, in general, normal loading, shear loading in partial slip and bulk tension. In very general terms, the magnitude of the state of stress in this region (Fig. 5), may be less severe than it is at remote points in a corresponding finite contact. This is in stark contrast to complete contacts, where the contact edge is a singular point, and hence the asymptotes are themselves singular, decaying, usually, to zero at infinitely remote points from the contact corner. The point is made because, for an incomplete contact, the solutions are locally correct, but diverge at remote points; this is an acceptable limitation of the solutions, because they are required to model only the local behaviour.

Details of the solutions are given in Dini, Hills and Sackfield; [7,8] the first develops the theory *ab initio*, whilst the second includes detailed considerations of shakedown, bulk tension and internal properties of the asymptote. For brevity, only the results are given here. The contact pressure, $p(t)$, is represented by the distribution

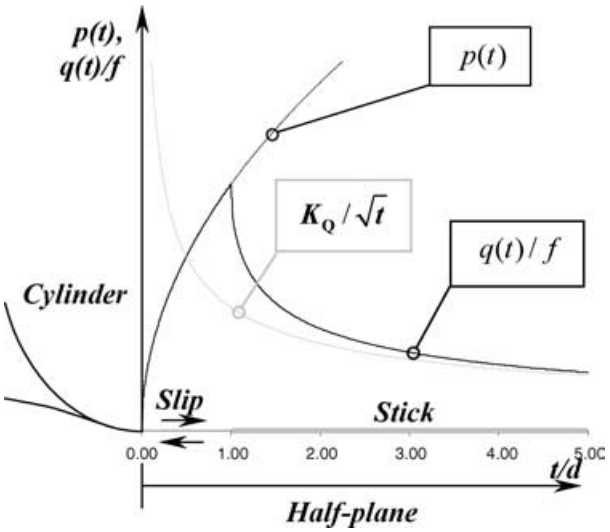

Fig. 5 Bounded asymptote for partial slip contacts. Here d is the portion of contact undergoing partial slip.

$$\begin{aligned} p(t) &= K_P\sqrt{t} \quad t > 0 \\ &= 0 \qquad t < 0, \end{aligned} \quad (9)$$

where the mode I generalised stress intensity factor K_P has dimensions $[FL^{-5/2}]$, and may be found by matching the local state of stress at the edge of any finite contact to the form implied by the asymptote. If the extent of the slip zone is d, the shearing traction, $q(t)$, may be written in the form

$$\begin{aligned} q(t) &= \frac{2K_Q}{d}\sqrt{t} && 0 < t < d \\ &= \frac{2K_Q}{d}(\sqrt{t} - \sqrt{t-d}) && t > d \\ &= \frac{K_Q}{\sqrt{t}} && t \gg d \\ &= 0 && t < 0, \end{aligned} \quad (10)$$

where the mode II generalised stress intensity factor K_Q has dimensions $[FL^{-3/2}]$, and continuity of tractions at the stick–slip interface indicates that

$$\frac{K_Q}{K_P} = \frac{fd}{2}. \quad (11)$$

The whole point of deducing the family of solutions described above is, of course, to provide a completely portable stress environment that may be matched into the edge of any incomplete contact problem. In this paper, they will be used with Hertzian contacts. Figure 6 shows a Hertzian contact, suffering partial slip, and subject to tension, σ_b, in the form it is usually encountered in a FF test. For simplicity, here, it is assumed that the contacting body

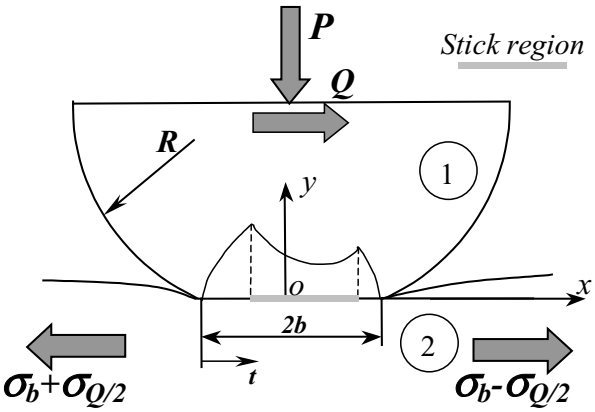

Fig. 6 Hertzian contact: partial slip configuration in the presence of remote bulk tension.

is sufficiently thick for half-plane theory to be appropriate (although this is not essential for the whole process to be valid), and for the contact to extend to $(-b \le x \le b)$. The central region is stick (but not symmetrically, because of the effect of the tension), while the outer regions are in slip. With the shearing force having the sense shown, the critical region for the nucleation of cracks, is the trailing edge of the contact, and the values of the stress intensity factor may be found by taking the contact pressure and shearing traction distributions induced by various contact conditions, and matching them to the forms implied by the asymptotes, *viz.*

$$\boldsymbol{K}_{\mathrm{P}} = \lim_{t\to 0} \frac{\boldsymbol{\sigma}_{\mathrm{yy}}}{\sqrt{\boldsymbol{t}}},$$
$$\boldsymbol{K}_{\mathrm{Q}} = \boldsymbol{f}\boldsymbol{d}\boldsymbol{K}_{\mathrm{P}}/2. \tag{12}$$

These give[**]

$$\boldsymbol{K}_{\mathrm{P}} = \frac{2\sqrt{2}\boldsymbol{P}}{\boldsymbol{\pi}\sqrt{\boldsymbol{b}^3}},$$
$$\boldsymbol{K}_{\mathrm{Q}} = \frac{\sqrt{2}\boldsymbol{f}\boldsymbol{P}}{\boldsymbol{\pi}\sqrt{\boldsymbol{b}}}\left\{1 + \frac{\boldsymbol{\sigma}_{\mathrm{b}}\boldsymbol{\pi}\boldsymbol{b}}{8\boldsymbol{f}\boldsymbol{P}} - \sqrt{1 - \frac{\boldsymbol{Q}}{\boldsymbol{f}\boldsymbol{P}}}\right\}. \tag{13}$$

Thus, the state of stress adjacent to the nucleation region in the well-known Hertzian FF tests can be encapsulated in these two constants. The spatial distribution of stress is given by the sum of the corresponding Muskhelishvili's potentials, and their variation with time.[7,8]

Going back to the CLNA formulation, applying the solution obtained by Dini, Hills and Sackfield[7,8], in the most general case for Hertzian contact under constant normal load, but oscillating in phase bulk and tangential loads, the equivalent geometrical factor is obtained as

$$\boldsymbol{Y}_{\mathrm{FF,\,Dini}}\left(\boldsymbol{\sigma}_{\mathrm{b}}, \overline{\boldsymbol{p}}, \boldsymbol{f}, \frac{\boldsymbol{Q}}{\boldsymbol{P}}\right) = \frac{4}{\sqrt{2\pi}}\boldsymbol{Y}_{\mathrm{FF,\,slip}}\left(1 - \sqrt{1 - \boldsymbol{Q}/\boldsymbol{f}\boldsymbol{P}}\right) + \frac{1}{2\sqrt{2\pi}}. \tag{14}$$

Note that the original $Y_{\mathbf{FF}}$ can be written as

$$\boldsymbol{Y}\left(\boldsymbol{\sigma}_{\mathrm{b}}, \overline{\boldsymbol{p}}, \boldsymbol{f}, \frac{\boldsymbol{Q}}{\boldsymbol{P}}\right) = \boldsymbol{Y}_{\mathrm{FF,\,slip}}\boldsymbol{Q}/\boldsymbol{f}\boldsymbol{P} + \frac{1}{2\gamma}. \tag{15}$$

At $Q/fP = 0$, we get respectively,

$$\boldsymbol{Y}_{\mathrm{FF,\,Dini}} = \frac{1}{2\sqrt{2\pi}} \quad \text{and} \quad \boldsymbol{Y}_{\mathrm{FF,\,stick}} = \frac{1}{2\gamma}, \tag{16}$$

and these hardly differ since for $\gamma = 2$ the numerical values are 1/5 and 1/4 (the coefficient $Y_{\mathrm{FF,\,Dini}}$ is here slightly lower than the $Y_{\mathrm{FF,\,stick}}$ in the original CLNA theory). It is clear that the two formulations differ since the details of the geometry mainly affects the transition from stick to slip in the contact areas, and in turn this is particularly important when the frictional tractions are highest with respect to the bulk load, and when they occur near the edge of the contact, i.e. near full sliding. In fact, the largest differences occur when *Q/fP* approaches unity, when $Y_{\mathrm{FF,\,Dini}} = \frac{4}{\sqrt{2\pi}}Y_{\mathrm{FF,\,slip}} + \frac{1}{2\sqrt{2\pi}} \cong 1.6Y_{\mathrm{FF,\,slip}} + 0.2$, and hence $\frac{Y_{\mathrm{FF,\,Dini}}}{Y_{\mathrm{FF}}} \cong \frac{1.6Y_{\mathrm{FF,\,slip}}+0.2}{Y_{\mathrm{FF,\,slip}}}$, which clearly is particularly large for low $Y_{\mathrm{FF,\,slip}}$, and then tends to 1.6 (the coefficient $Y_{\mathrm{FF,\,Dini}}$ being always lager). This indicates that the $Y_{\mathrm{FF,\,Dini}}$ crosses the original Y_{FF} for a given *Q/fP*, and then becomes larger than the original Y_{FF}. In terms of relative percentage error again for $Q/fP = 1$, i.e. near full slip $\frac{Y_{\mathrm{FF}} - Y_{\mathrm{FF,\,Dini}}}{Y_{\mathrm{FF,\,Dini}}}100 \cong \frac{-0.6Y_{\mathrm{FF,\,slip}} - 0.2}{1.6Y_{\mathrm{FF,\,slip}} + 0.2}100$ (Fig. 7), it is clear that the error[†] we made in the original Y_{FF} can be considered as a underestimate (for the limit case of $Q/fP = 1$) of up to 100% (for negligible $Y_{\mathrm{FF,\,slip}}$) or to a mere overestimate of 37.5% for very large $Y_{\mathrm{FF,\,slip}}$. Clearly, the old CLNA is conservative at small *Q/fP* ratios, and underconservative near full slip.

Figure 8 gives a complete picture of the results in partial slip, for $Y_{\mathrm{FF,\,slip}} = 0.5,1,2$, where it is clear that a significant discrepancy only occurs near the full sliding case. In the intermediate ranges of *Q/fP* (quite commonly used for experimental analyses as describing realistic loading conditions) the results are similar, as it is made clear in Fig. 8b, where the relative error is found to lay within a mismatch range of ±20% for intermediate load ratios ranging between 0.25 and 0.75. Nevertheless, the difference in the refined model is considerable.

[**]Note that the analytical formula is only rigorously valid for moderate values of bulk loads. A numerical value for K_Q needs to be computed numerically for large value of remote bulk stress[11].

[†]We write 'error' here, assuming the present formulation is more refined. As discussed in the introduction, however, this is not necessarily the case.

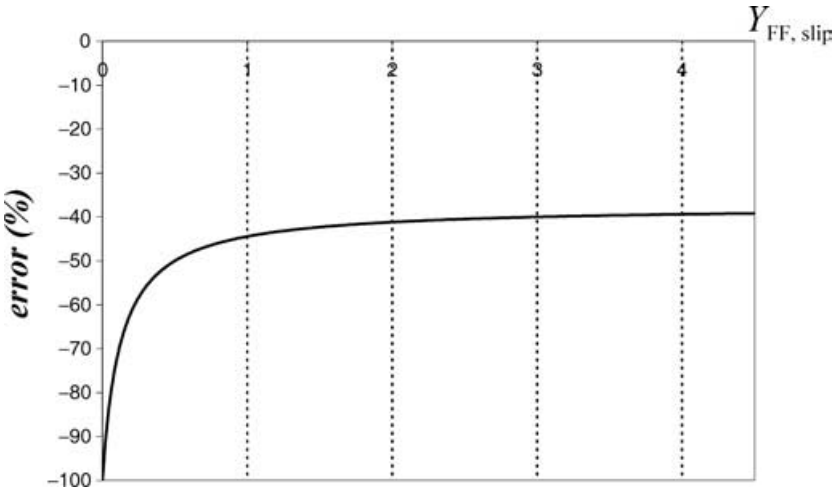

Fig. 7 The relative percentage error for $Q/fP = 1$, i.e., $\frac{Y_{FF} - Y_{FF,\,Dini}}{Y_{FF,\,Dini}} 100 \cong \frac{-0.6 Y_{FF,slip} - 0.2}{1.6 Y_{FF,\,slip} + 0.2} 100$ near full slip, as a function of $Y_{FF,\,slip}$. This is where the error is largest, and gives the upper bound for partial slip conditions.

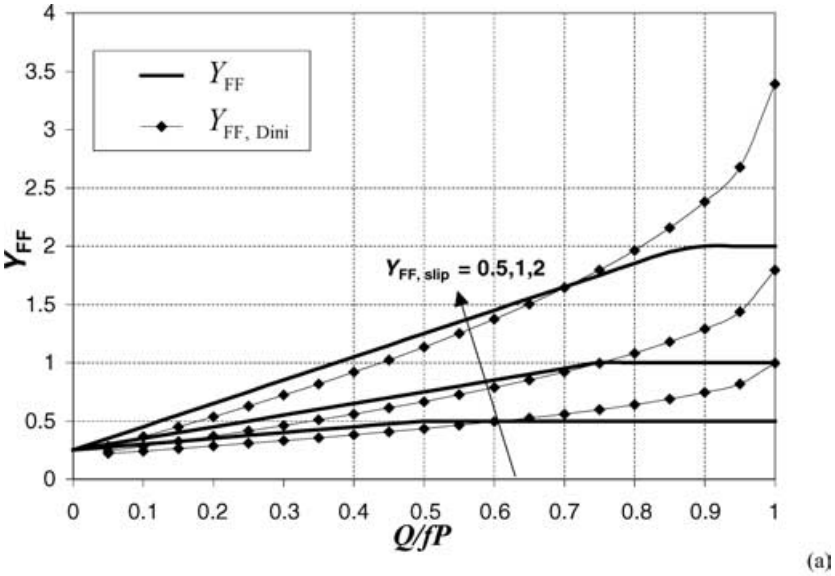

(a)

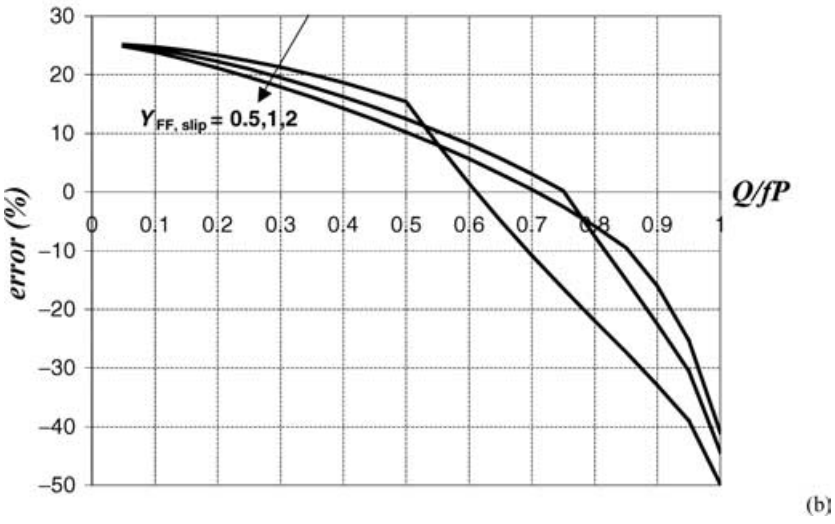

(b)

Fig. 8 Partial slip: the original fretting fatigue CLNA *fictitious geometrical factor* from Eq. (6), compared with the new Y_{Dini} factor, given in Eq. (14), for three example cases with $Y_{slip} = 0.5,1,2$. (a) absolute values (b) percentage error in the original CLNA formulation with respect to the present one. Clearly, the old CLNA is conservative at small Q/fP ratios, and underconservative near full slip.

Moving to the 'large blunt notch' equivalent fretting problem, we follow the original CLNA model, as the asymptotic theory does not help here. In order to find the equivalent fretting stress concentration factor, K_{ft}, and hence define the (horizontal) threshold for large contacts, we need a good estimate of the peak stress. A number of exact results are known from detailed analyses (Ciavarella *et al*.[10,12]), and in particular a simple (but yet accurate) formula for Hertzian, or rounded flat geometry, subject to constant pressure and oscillating tangential load is

$$\sigma_{\max} = \sigma_b + \sigma_{\text{cont}} = \sigma_b + \frac{8}{\pi}\overline{p}k\sqrt{fQ/P}. \tag{17}$$

Here k is a contact geometrical factor equal to *one* in the Hertz contact case, and increasingly greater for rounded flat geometries towards the flat indenter case. The above formula is only exact when no bulk stress is considered, and an approximate, linear superposition is used here for simplicity, in the general case. In terms of the non-dimensional ratios

$$K_{\text{ft}}\left(\frac{\overline{p}}{\sigma_b}, \frac{Q}{P}, f, k\right) = 1 + \frac{8}{\pi}\frac{\overline{p}}{\sigma_b}k\sqrt{f\frac{Q}{P}}, \tag{18}$$

showing that K_{ft} depends on all three non-dimensional factors, plus a geometrical factor, but obviously does not depend on the size of the contact. Finally, for full sliding, $Q = fP$, the stress concentration reaches the maximum value. Figure 9 shows an example plot of the stress concentration factor K_{ft}. It should be noted that for full sliding on a Hertzian contact,

$$K_{\text{ft,lim}}\left(\frac{\overline{p}}{\sigma_b}, f\right) = 1 + \frac{8}{\pi}\frac{\overline{p}}{\sigma_b}f, \tag{19}$$

and hence we can write the K_{ft} as a function of the limit full sliding value for Hertzian contact as

$$K_{\text{ft}}\left(\frac{\overline{p}}{\sigma_b}, \frac{Q}{P}, f, k\right) = 1 + \left[K_{\text{ft,lim}}\left(\frac{\overline{p}}{\sigma_b}, f\right) - 1\right]k\sqrt{\frac{Q}{fP}}. \tag{20}$$

The former shows that the effect of partial slip on K_{ft} is different from that of the Y_{FF} factor in the CA model above (see Fig. 8). This shows, in fact, a square-root dependence on Q/fP, whereas Y_{FF} follows a linear variation followed by a constant function of Q/fP. This difference will, therefore, cause a different effect of partial slip in the CA and in the NA regimes, suggesting that the transition point will not occur at a constant value. In particular, the curves in Fig. 9 show the variation of K_{ft} as a function of Q/fP for $K_{\text{ft,lim}}(\frac{\overline{p}}{\sigma_b}, f) = 3,5,9$, and for Hertzian geometry, i.e. $k = 1$.

By equating the K_{ft} with the K_{ff} predictions we get an estimate of the size separating the 'crack-like' from the 'blunt notch' behaviours. However, this is not described in detail in this paper for brevity.

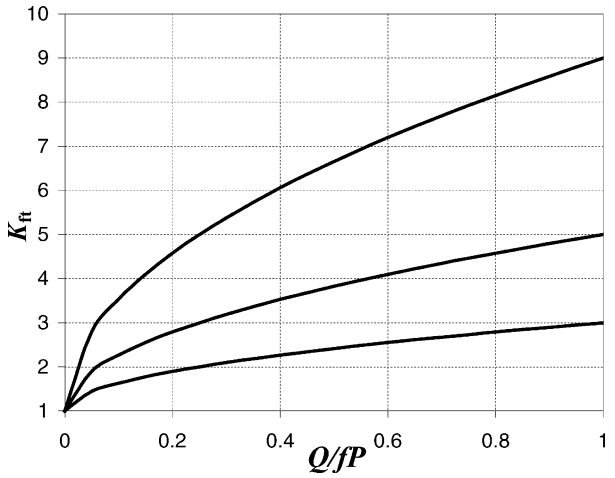

Fig. 9 Partial slip: the fretting fatigue stress concentration factor K_{ft}, given approximately by Eq. (20). Here represented are three cases, with Hertzian geometry ($k = 1$), showing the effect of partial slip on K_{ft} for $K_{\text{ft,,lim}}(\frac{\overline{p}}{\sigma_b}, f) = 3, 5, 9$.

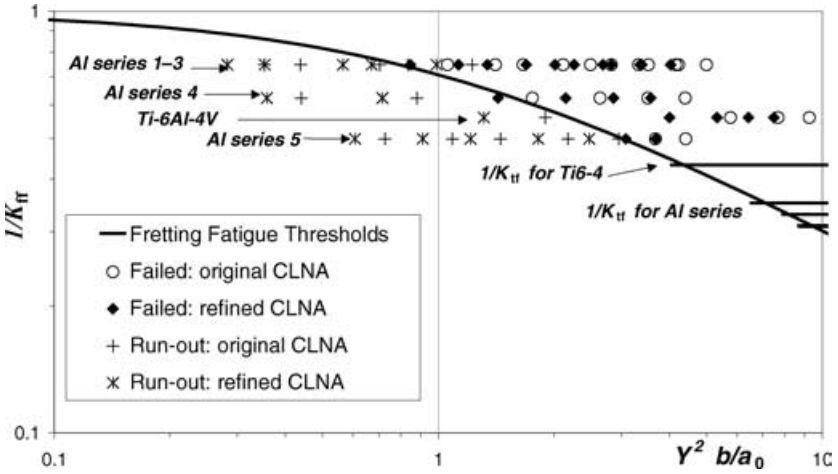

Fig. 10 Comparison of Nowell co-workers' experiments[13,14] ($a_0 = 91$ μm, 25 μm for Al- and Ti-alloys, respectively, with predictions of both the original and the refined CLNA model.

Turning now to the validation of the model, in the original paper[2] Ciavarella presented the data of experimental results in the literature. Here, we simply repeat the comparison for the classical Hertzian results of Nowell and coworkers[13,14] (see Fig. 10). Details of materials, geometries and loading conditions used to generate the data set are given by Araújo and Nowell[14] and are also summarised in Tables 1–3.

In the plot of Fig. 10, the x-axis is $Y_{FF}{}^2 b/a_0$. This makes the El Haddad curve of the (fretting equivalent) Atzori–Lazzarin diagram a single curve, and only the blunt notch behaviour may change. It should be noted that the introduction of the corrective term Y_{FF} does not corespond to a significant improvement of the data fit. In fact, only two data points are particularly affected by the refinement. On one hand, one of the tests from Al series 1–3, which was not falling in the area of the plot indicating safe life according to the original CLNA model, moves closer to the threshold curve, hence indicating an improvement of the prediction achieved using the refined model. On the other hand, one of the tests from Al series 4, which seemed to lay on the right region of the diagram according to the original CLNA prediction, moves to the other area of the plot. Evidently the data set available for this geometry is not sufficient to estimate the improvement induced by the embedment of the asymptotic formulation within the CLNA model. This is because most of the data generated in literature using cylindrical indenters are not thought of as a way to determine the FF threshold (see for example Szolwinski and Farris[15] where all the specimen were broken within 10^6 cycles) and the difference between the two methods is almost negligible for the data set presented here. Further experiments using Hertzian geometry should be carried out to assess the improvement introduced by the new formulation.

However, in order to explore the differences between the original and the new formulation and, hence, help to devise experimental tests that should shed some light on this issue, we can now show the effect of changing the various parameters directly on a single diagram. Instead of plotting the $1/K_{ff}$ factor as a function of $Y_{FF}{}^2 b/a_0$, which makes the El Haddad curves collapse, we plot the diagram as a function of b/a_0 only, and change the load parameters in different manners. In Fig. 11(a), we keep $R_q = Q/P$ constant and equal to the friction coefficient f, so that full sliding is obtained, but for different values $f = 0.2,0.4,0.6,0.8,1$. The geometry is Hertzian and the pressure factor $Rp = \frac{\bar{p}}{\sigma_b} = 1$. The difference between the

Table 1 Mechanical properties of Al4%Cu and T1–6Al-4V

Material	Young modulus E (GPa)	Poisson's ratio, n	0.2% yield strength (MPa)
Al4%Cu	74	0.33	465
Ti-6Al-4V	110	0.32	974

Table 2 Experimental parameters used in the fretting fatigue tests

Material	Peak pressure p_0 (MPa)	Q/P	σ_b (MPa)	Friction coefficient, f
Al Series 1	157	0.45	92.7	0.75
Al Series 3	143	0.45	92.7	0.75
Al Series 4	143	0.45	77.2	0.75
Al Series 5	120	0.45	61.8	0.75
Ti-6Al-4V	650	0.16	280	0.55

Table 3 Geometrical properties and fretting fatigue total life

Al Series 1								
Pad radius, R (mm)	12.5	25	37.5	50	75	100	125	150
Contact half-width, b (mm)	0.10	0.19	0.28	0.38	0.57	0.76	0.95	1.14
Life (10^6 cycles)	>10	>10	>10	1.29	0.67	0.85	0.73	0.67
Al Series 3								
Pad radius, R (mm)	12.5	25	37.5	50	75	100	125	150
Contact half-width, b (mm)	0.09	0.18	0.27	0.36	0.54	0.72	0.9	1.08
Life (10^6 cycles)	>10	>10	4.04	1.50	0.80	0.61	1.24	0.69
Al Series 4								
Pad radius, R (mm)	12.5	25	50	75	100	125		
Contact half-width, b (mm)	0.09	0.18	0.36	0.54	0.72	0.9		
Life (10^6 cycles)	>10	>10	1.2	1.42	0.61	1.24		
Al Series 5								
Pad radius, R (mm)	25	37.5	50	75	100	125	150	
Contact half-width, b (mm)	0.14	0.21	0.28	0.42	0.57	0.71	0.85	
Life (10^6 cycles)	>10	>10	>10	>10	>10	1.57	1.23	
Ti-6Al-4V								
Pad radius, R (mm)	25	37.5	50	60	70			
Contact half-width, b (mm)	0.25	0.76	1.01	1.22	1.42			
Life (10^5 cycles)	>14	5.21	3.74	1.96	1.73			

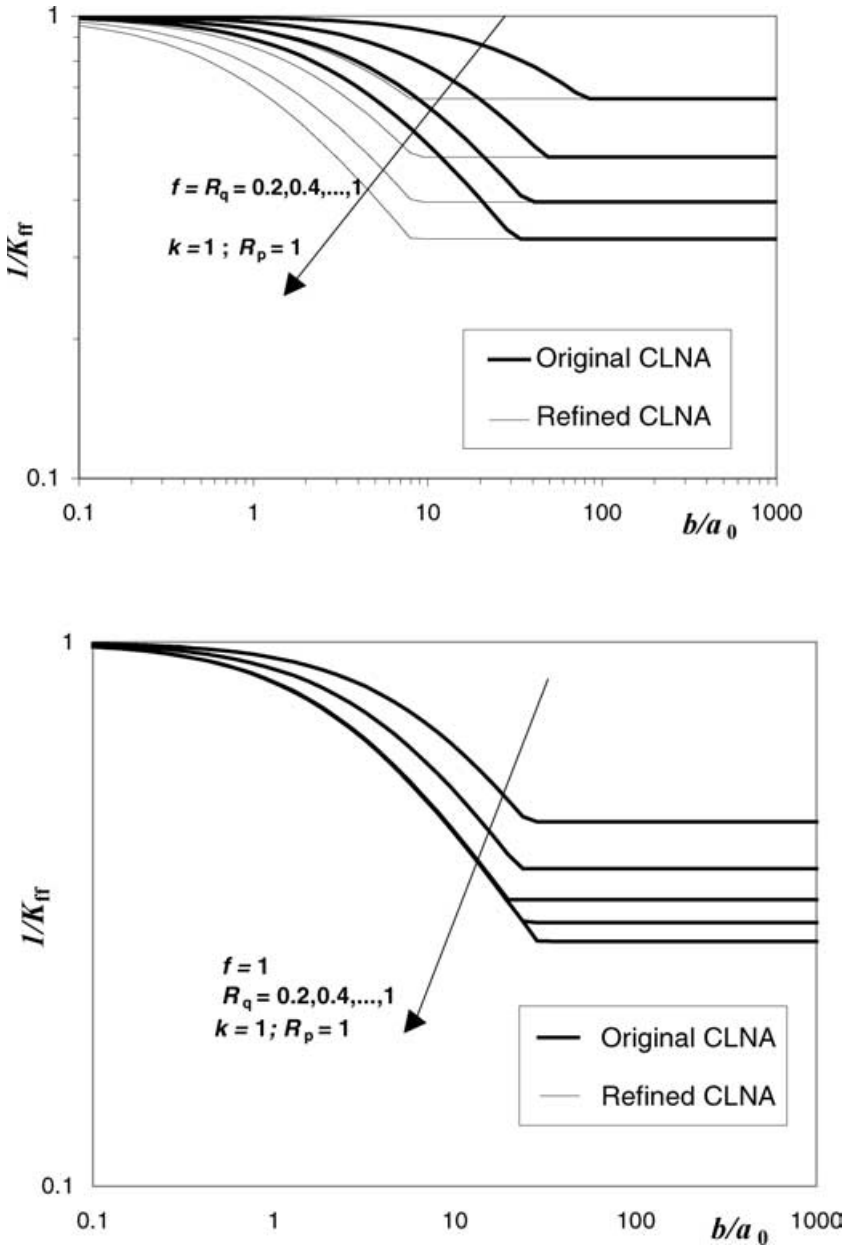

Fig. 11 The effect of varying $R_q = f$ (a) (while $R_p = 1$), or only $R_q = Q/P$ (b) (while $Rp = 1$ and $f = 1$), in the CLNA diagram using the original Y_{FF} or the new improved version $Y_{FF,\,Dini}$.

original and the improved CLNA model is large, because $R_q/f = Q/fP$ is large.

In the Fig. 11(b), we fix friction coefficient, and equal to *one*, but we vary the factor $R_q = Q/P = 0.2,0.4,0.6,0.8,1$. Here, we clearly see that the difference is smaller for the lower R_q ratios.

Furthermore, in Fig. 12(a), the effect of changing the R_p factor is shown, where $R_q = 1$ and $f = 1$, and the difference is large again. Fig. 12(b) keeps $R_q = 0.2$ and $f = 1$, but vary the pressure ratio, showing the largest effect of all, and a small difference with respect to the original treatment, as expected. Finally, Fig. 13 shows the effect of varying f, while $R_q = 0.2$ and $R_p = 1$, and hence the $R_q/f = Q/fP$ factor changes again, showing initially larger differences than for the final case, where Q/fP is only 0.2.

Some of these loading conditions would represent ideal test configurations to assess the improvement of the methodology and check the accuracy of the new formulation with respect to the original model.

DISCUSSION

As we have seen, the older CLNA model is more conservative than the 'refined' model at small Q/fP ratios, and,

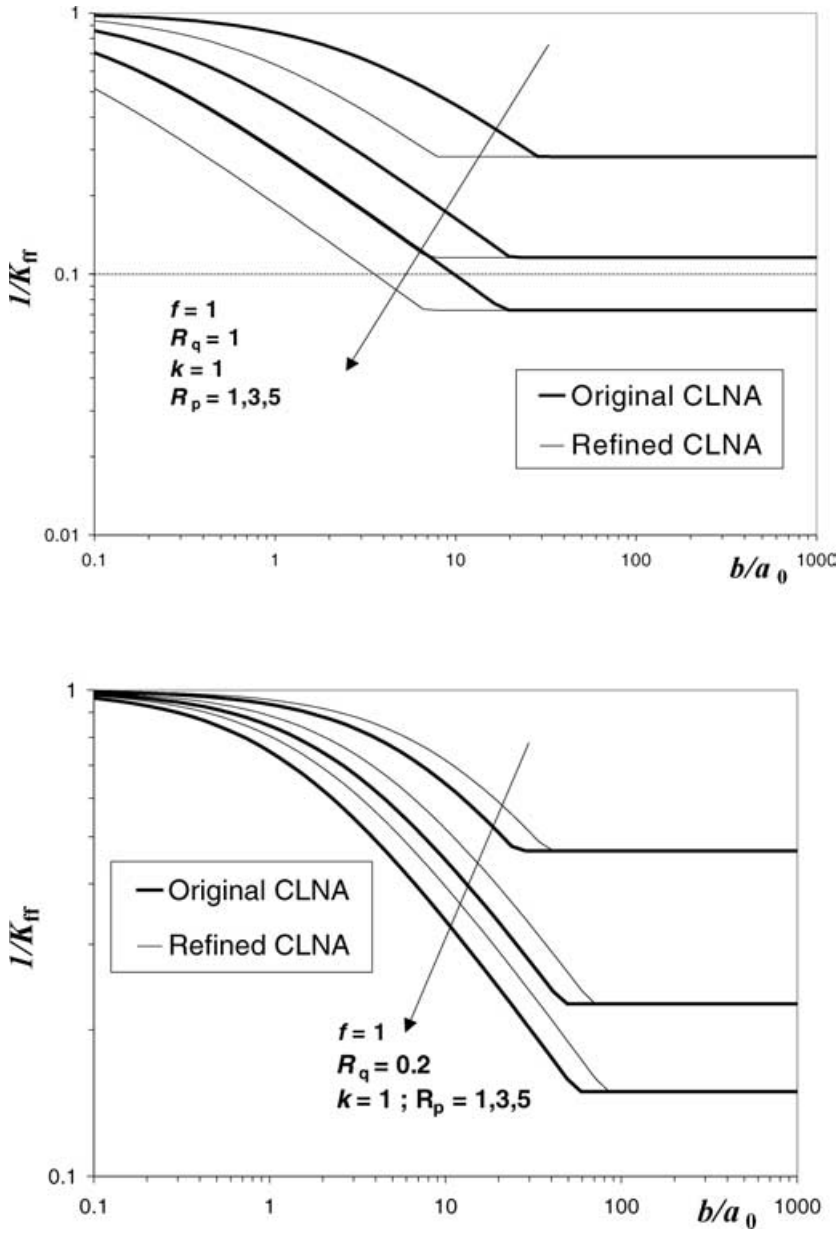

Fig. 12 The effect of varying $Rp = \frac{\overline{p}}{\sigma_0}$ (a) (with $R_q = 1$) or (b) with $R_q = 0.2$ and $f = 1$, in the CLNA diagram, using the original Y_{FF} or the new improved version $Y_{FF,\,Dini}$.

viceversa, less conservative near full slip. Hence, the correction is suggested, lacking a definitive answer over which criterion is more reliable, near full slip. The difference really comes from the way the asymptotes are found. In the old CLNA model, the geometry is abruptly approximated with a flat one, and this geometry has a very simple response in terms of stress intensity factors. A little more complicated is to understand how the asymptotic method of Dini, Hills and Sackfield works; essentially, because the geometry is locally bounded, the shear tractions near the edges are very limited, and in order to support the given total load, the stress intensity factor, which is a measure of the strength of the stress field at the transition stick to slip, needs to be larger and continues to grow up to full sliding. This is the reason behind the differences. Now, as we have briefly mentioned already in the Introduction, the real problem has probably not much to do with either of the formulations! In fact, both approaches tend to simplify the problem of fatigue crack initiation or early propagation and self-arrest. This problem would be probably best formulated by actually considering a small crack in the contact edge zone, and computing the stress intensity factors experienced. Naturally, following the evolution of this actual crack would be extremely difficult; not only we would need to compute the stress intensity factors, also depending on the possible orientation of this crack,

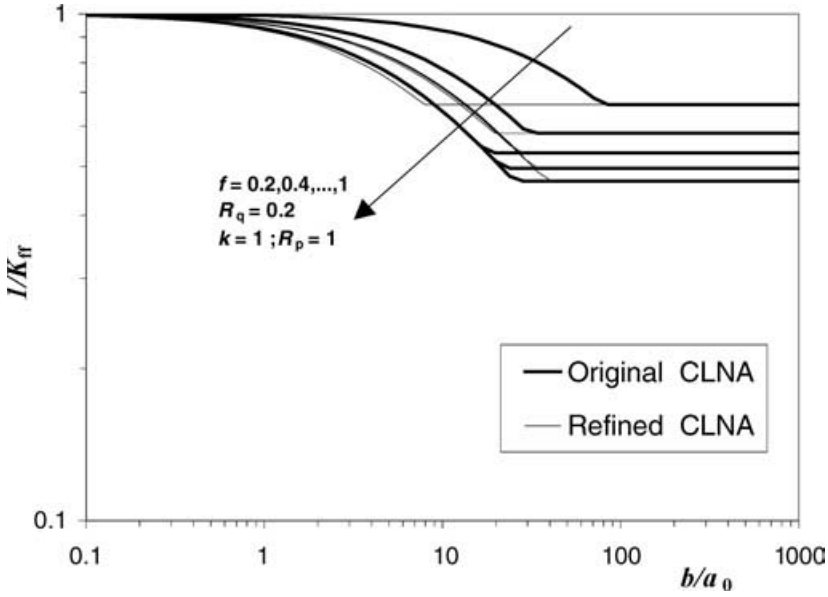

Fig. 13 The effect of varying f (with $R_q = Q/P = 0.2$ and $Rp = \frac{\overline{p}}{\sigma_b} = 1$ in the CLNA diagram, using the original Y_{FF} or the new improved version $Y_{FF,\ Dini}$.

immersed in the entire stress field (which we would then need to compute in detail), but its presence would affect slightly the contact traction distributions. Also, the initiation/early propagation would be that of a short crack which depends on many other factors than those considered here, including plasticity at the crack tip, and microstructural parameters. However, certainly from the geometrical point of view, it is very likely that the details of the geometry of the contact near the edge would loose importance and it is unclear if either of the parameters found in the original CLNA model, or the new refined model, would be most correct.

One additional advantage of the original CLNA model was that the crack-like behaviour reduced all possible geometries to a single contact problem, whereas the new refined model predicts a certain dependence on the actual contact geometry. We have only studied here the Hertzian geometry, which is perhaps the most interesting and the one for which many data are available. Also, it is quite remote from the flat geometry, and hence it was interesting to see how large the differences were in the two asymptotics. Admittedly, we found the difference much smaller than expected. However, in many components, a much flatter geometry is often used (flat or rounded-flat geometries). It would be interesting to compare if the actual threshold in experiments depends significantly on geometry alone or not, but to the best of the authors' knowledge, there are no appropriate data so far. In those cases, however, the differences in the two models would be much smaller than what found here and hence, the original CLNA model, for its simplicity, remains a very convenient simple closed form criterion.

CONCLUSIONS

An improvement of the original CLNA model has been suggested, where the stress field asymptotics extracted by Dini, Hills and Sackfield[7,8] have been used instead of the crude 'sharp' geometry approximation adopted in the original CLNA model. The differences in the 'fretting fatigue' equivalent Y corrective factor, Y_{FF}, for the generalised mode II stress intensity range have been found, and have been shown to be *small* except near the full sliding limit. In particular, the percentage error can vary in principle between +25% and −100%, the former limit being constant and at low Q/fP ratios, the second limit depending on the Y_{FF} factor in full sliding, where the new criterion would be more conservative and is hence suggested. A comparison with the classical Nowell and coworkers[13,14] experiments in the literature does not permit to judge if better agreement with this correction with respect to the original formulation is achieved. New tests using different loading conditions have, therefore, been proposed for future validation of the improved accuracy of the method. Clearly, in flatter geometries than Hertzian, we do not expect the refinements using asymptotics would be significant, and we therefore maintain the original CLNA model as a convenient alternative.

REFERENCES

1 Atzori, B. and Lazzarin, P. (2001) Notch sensitivity and defect sensitivity under fatigue loading: two sides of the same medal. *Int. J. Fract.* **107**, L3–L8.

2 Ciavarella, M. (2003) A crack-like notch analogue (CLNA) for a safe-life fretting fatigue design methodology. *Fat. Fract. Engng. Mat. Struct.* **26**, 1159–1170.
3 Atzori, B., Lazzarin, P. and Meneghetti, G. (2003) Fracture mechanics and notch sensitivity. *Fat. Fract. Engng. Mat. Struct.* **26**, 257–267.
4 El Haddad, M. H., Topper, T. H. and Smith, K. N. (1979) Prediction of non-propagating cracks. *Engng. Fract. Mech.* **11**, 573–584.
5 Ciavarella, M. and Meneghetti, G. (2004) On fatigue limit in the presence of notches: classical vs. recent formulations. *Int. J. Fat.* **26**, 289–298.
6 Giannakopoulos, A. E., Lindley, T. C. and Suresh, S. (1998) Overview N. 129, Aspects of equivalence between contact mechanics and fracture mechanics: theoretical connections and a life-prediction methodology for fretting-fatigue. *Acta Mater.* **46**, 2955–2968.
7 Dini, D. and Hills, D. A. (2004) Bounded asymptotic solutions for incomplete contacts in partial slip. *Int. J. Solids Struct.* **41**, 7049–7062.
8 Dini, D., Sackfield, A. and Hills, D. A. (2005) Comprehensive bounded asymptotic solutions for incomplete contacts in partial slip. *J. Mech. Phys. Solids*. **53**, 437–454.
9 Ciavarella, M. and Macina, G. (2003a) A note on the crack analogue model for fretting fatigue, *Int J Solids Struct*. **40**, 807–825.
10 Ciavarella, M. and Macina, G. (2003b) New results for the fretting-induced stress concentration on Hertzian and flat rounded contacts. *Int J. Mech. Sci.* **45**, 449–467.
11 Nowell, D. and Hills, D. A. (1987) Mechanics of fretting fatigue. *Int J. Mech. Sci.* **29**, 355–365.
12 Ciavarella, M., Macina, G. and Demelio, G. P. (2002) On stress concentration on nearly flat contacts. *J Strain Anal Eng*. **37**,493–501.
13 Nowell, D. (1988) An analysis of fretting fatigue. D. Phil. thesis. University of Oxford.
14 Araújo, J. A. and Nowell, D. (2002) The effect of rapidly varying contact stress fields on fretting fatigue. *Int. J. Fat.* **24**, 763–775.
15 Szolwinski, M. P. and Farris, T. N. (1998) Observation, analysis and prediction of fretting fatigue in 2024-T351 aluminum alloy. *Wear*. **221**, 24–36.